Journal of Heat and Mass Transfer, Vol. 24, Aug. 1981, pp. 1345–1357.

[4]Saitoh, T., "Numerical Methods for Multidimensional Freezing in Arbitrary Domains," *ASME Journal of Heat Transfer,* Vol. 100, May 1978, pp. 294–299.

[5]Duda, J. L., Malone, M. F., Notter, R. H., and Vrentas, J. S., "Analysis of Two Dimensional Diffusion-Controlled Moving Boundary Problems," *International Journal of Heat and Mass Transfer,* Vol. 18, May 1975, pp. 901–910.

[6]Shamsunder, N., and Rooz, E., "Numerical Methods for Moving Boundary Problems," *Handbook of Numerical Heat Transfer,* Wiley, New York, 1988, pp. 747–786.

Parallel-Flow and Counter-Flow Conjugate Convection from a Vertical Insulated Pipe

J. Libera* and D. Poulikakos†
University of Illinois at Chicago, Chicago, Illinois 60680

Nomenclature

A = dimensionless group, Eq. (22)
B = dimensionless group, Eq. (6)
c_{pl} = specific heat of pipe fluid
g = acceleration of gravity
H = length of pipe
h = heat-transfer coefficient
K = permeability of porous material
k = thermal conductivity
Nu = Nusselt number
Pe = Peclet number, Eq. (8)
Pr = Prandtl number
q = heat flux perpendicular to flow direction
R = radius of pipe
r = radial direction, Fig. 1
Ra_κ = Darcy modified Rayleigh number, Eq. (13)
T_1 = mean temperature of the pipe fluid, $2/R_i^2U\int_0^{R_i}u_1t_1r\,dr$
T_2 = temperature of the fluid in the insulation
t_1 = temperature
U = mean velocity of pipe fluid
u = velocity component in the x direction
v = velocity component in the y direction
x = coordinate parallel to flow direction
y = coordinate perpendicular to flow direction
α = thermal diffusivity of pipe fluid
β = coefficient of thermal expansion
λ = Oseen function
ν = kinematic viscosity
ρ = fluid density
θ = dimensionless temperature

Subscripts
c = cold
i = inner surface of pipe
o = outer surface of pipe
w = pipe wall
$*$ = dimensional variable
∞ = reservoir condition far away from the pipe
1 = pipe fluid
2 = reservoir fluid

Received Jan. 5, 1989; revision received Sept. 25, 1989.

*Research Assistant, Department of Mechanical Engineering.
†Associate Professor, Department of Mechanical Engineering.

Introduction

CONJUGATE heat transfer finds numerous applications in thermal engineering. It is because of this reason that conjugate heat transfer has been the main focal point in several investigations over the past few decades. Since convection is a common heat-transfer mode, it is reasonable to expect that it often constitutes one of the two or more interweaving modes (mechanisms) in conjugate heat-transfer applications. For example, Poulikakos[1] studied theoretically the problem of natural convection along a vertical conductive wall coupled with film condensation on the other side of this wall. He determined the parametric domain over which the two coupled phenomena (natural convection and condensation) seriously affect each other as well as the overall heat transfer through the wall. In a related study, Poulikakos and Sura[2] investigated the interaction between condensation inside a vertical layer of insulation and natural convection at the surface of the insulation. Faghri and Sparrow[3] examined theoretically the coupling of condensation on a pipe and forced convection of a fluid inside the pipe. Also theoretical is the work of Bejan and Anderson,[4,5] who investigated the problem of natural convection along the impermeable interface of two fluid reservoirs[4] and a porous and fluid reservoir,[5] respectively. In the work of Bejan and Anderson,[4,5] the coupling was between two different counter-flowing boundary layers.

The present Note investigates the problem of interaction (coupling) of forced convection inside a vertical pipe and natural convection outside the pipe, where the pipe is surrounded by permeable insulation. This analysis finds applications in the design of insulation jackets for pipes, where the insulation can be modeled as an isotropic porous medium. It also provides the means for calculating heat-transfer gains or losses from a buried vertical pipe. Both the cases of counter flow and parallel flow are considered. Clearly, the heat transfer through the pipe wall is a direct result of the interaction between the forced convection inside the pipe and the natural convection outside the pipe.

Formulation and Analysis

Consider the system shown in Fig. 1a. A warm fluid is flowing inside a vertical conductive pipe opposite to the direction of gravity. The pipe is surrounded by a porous material saturated with a colder fluid, which is assumed to be in thermal equilibrium with the porous matrix. The heating effect of the forced convection in the pipe is responsible for the establishment of temperature gradients inside the porous reservoir. These gradients in turn trigger a natural convection flow in the direction opposite to gravity. Clearly, the temperature of the fluid in the pipe varies along the flow passage as does the wall temperature and the temperature difference across the natural convection current, which is assumed to be of the boundary-layer type. Therefore, the local and overall heat transfer from the fluid in the pipe to the porous material depends on the preceding conjugate heat-transfer mechanisms (natural convection and forced convection). Figure 1b pertains to the same phenomenon just explained with the difference that the fluid in the pipe and the fluid in the reservoir are flowing in the opposite direction (counterflow configuration).

To formulate the problem mathematically, we will focus first on the forced-convection side and next on the natural-convection side of the parallel-flow configuration in Fig. 1a.

Forced Convection Inside the Pipe

At any axial position the heat-transfer rate from the forced-convection side through the pipe wall to the natural-convection side is

$$dq = \frac{2\pi k_w}{\ell n(R_i/R_o)}(T_{w_i} - T_{w_o})\,dx^* \tag{1}$$

The heat-transfer rate convected to the inner surface of the pipe over a length dx^* is

$$dq = 2\pi R_i h_i (T_1 - T_{w_i})\,dx^* \tag{2}$$

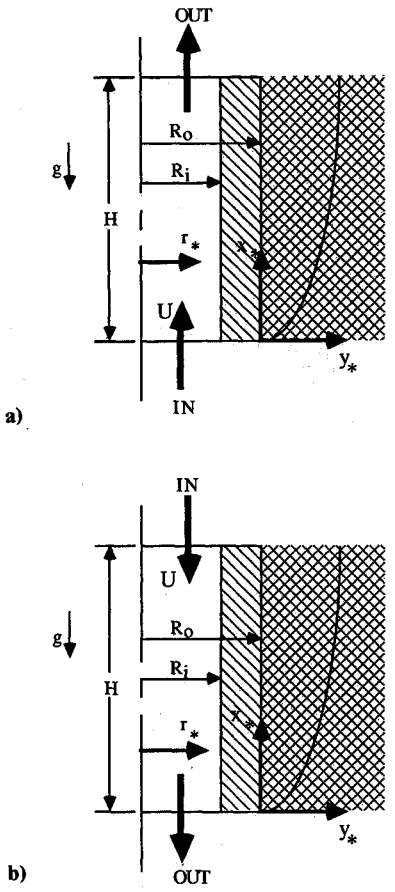

Fig. 1 Schematic of the system: a) cross section of the parallel-flow configuration; and b) cross section of the counter-flow configuration.

Next, stating that the heat-transfer rate leaving a volume of fluid of length dx^* in the pipe equals the heat-transfer rate convected to the inner surface of the pipe of length dx^* yields

$$m_1 c_{p1} \frac{dT_1}{dx^*} = 2\pi R_i h_i (T_1 - T_{w_i})\, dx^* \tag{3}$$

In the formulation above, the axial conduction in the fluid and the pipe wall have been neglected as is customarily done in pipe flow analyses. In addition, the turbulent heat-transfer coefficient for pipe flow h_i is assumed constant because of the fact that for turbulent pipe flows the thermal entrance length is very short and the coefficient is rather insensitive to the thermal boundary condition at the wall.[3] The preceding assumption is less valid for laminar pipe flow. All of the quantities in Eqs. (1-3), as well as in all of the equations to follow, are clearly defined in the nomenclature. Eliminating T_{w_i} from Eqs. (1-3) and casting the resulting equation in dimensionless form yields

$$\frac{d\theta_1}{dx} = -B(\theta_1 - \theta_0) \tag{4}$$

The nondimensionalization was carried out utilizing the following definitions:

$$x = \frac{x^*}{H}, \qquad \theta_1 = \frac{T_1 - T_c}{T_{1_i} - T_c}, \qquad \theta_0 = \frac{T_{w_o} - T_c}{T_{1_i} - T_c} \tag{5}$$

A dimensionless group appeared as a result of the nondimensionalization.

$$B = \left\{ Pe \left[\frac{R_i}{2H\, Nu_i} + \frac{R_i}{4H} \frac{k_1}{k_w} \ell n(R_o/R_i) \right] \right\}^{-1} \tag{6}$$

In Eq. (6), the Nusselt and the Peclet numbers are defined as

$$Nu_i = \frac{2h_i R_i}{k_1} \tag{7}$$

$$Pe = \frac{2UR_i}{\alpha_1} \tag{8}$$

Natural Convection in the Porous Material

The coordinate system for the following analysis is shown in Fig. 1. Following the Darcy flow model, the governing boundary-layer equations for natural convection in a porous medium for the given geometry can be written in dimensionless form as

$$\frac{\partial u}{\partial x} + \frac{\partial v}{\partial y} = 0 \tag{9}$$

$$\frac{\partial u}{\partial y} = \frac{\partial \theta_2}{\partial y} \tag{10}$$

$$u\frac{\partial \theta_2}{\partial x} + v\frac{\partial \theta_2}{\partial y} = \frac{\partial^2 \theta_2}{\partial y^2} \tag{11}$$

The following dimensionless parameters were used in addition to those already defined in Eq. (5):

$$y = y^*/\delta, \qquad u = u^*\delta^2/\alpha H$$

$$v = v^*\delta/\alpha, \quad \theta_2 = (T_2 - T_c)/(T_{1_i} - T_c), \quad \delta = HRa_\kappa^{-1/2} \tag{12}$$

where

$$Ra\kappa = \frac{g\beta KH}{\alpha\nu}(T_{1_i} - T_c) \tag{13}$$

is the Darcy-modified Rayleigh number based on the height H and overall temperature difference ΔT. The horizontal length scale δ was determined from a scale analysis as outlined by Weber.[6] In order to arrive at Eq. (10), the vertical and horizontal pressure gradients were eliminated from the Darcy momentum equations, and the Boussinesq approximation was then used to eliminate the density in favor of the temperature variable θ_2. According to the Boussinesq approximation, the density is assumed constant in all terms except the buoyancy term, where it is assumed to depend linearly on temperature $\{\rho = \rho_c[1 - \beta(T_2 - T_c)]\}$. The boundary conditions for the porous side complete the mathematical formulation of the problem.

At $y = 0$:

$$u = u_0, \qquad v = 0, \qquad \theta_2 = \theta_0(x) \tag{14}$$

At $y \to \infty$:

$$u = 0, \qquad \theta_2 = 0 \tag{15}$$

To obtain solutions for the equations governing fluid and energy transport in the porous material, we follow the Oseen linearization technique first demonstrated in natural convection analysis by Gill.[7] No details will be given here. All of the details are reported in references such as Poulikakos,[1] Poulikakos and Sura,[2] Bejan and Anderson,[5] and Libera.[8] The final expressions for the temperature and velocity distributions are

$$u = \theta_0 e^{-\lambda y} \tag{16}$$

$$\theta_2 = \theta_0 e^{-\lambda y} \tag{17}$$

In order to determine the unknown functions $\theta_0(x)$ and $\lambda(x)$, we require that Eqs. (16) and (17) satisfy Eq. (11) integrated

across the boundary layer, which amounts to satisfying the following integral equation:

$$\frac{d}{dx}\int_0^\infty u\theta_2\,dy + |\,v\theta_2\,|_0^\infty = \left|\frac{\partial\theta_2}{\partial y}\right|_0^\infty \tag{18}$$

Combining Eqs. (16–18), we derive the following differential equation relating the unknown functions $\theta_0(x)$ and $\lambda(x)$:

$$\frac{d}{dx}\left(\frac{\theta_0^2}{2\lambda}\right) - \lambda\theta_0 = 0 \tag{19}$$

To complete the analysis, we invoke the heat-flux matching condition at the outer surface of the pipe:

$$\frac{2\pi k_w\,dx^*}{\ell n(R_o/R_i)}(T_{w_i} - T_{w_o}) = -2\pi R_0\,dx^* k_2\left(\frac{\partial T_2}{\partial y^*}\right)_{y^*=0} \tag{20}$$

Eliminating T_{w_i} from Eq. (20), using Eqs. (1) and (2), and casting the result into dimensionless form yields

$$\frac{1}{A}(\theta_1 - \theta_0) = \lambda\theta_0 \tag{21}$$

where we have introduced a second dimensionless group A defined as

$$A = \left(\frac{4R_o}{R_i}\frac{k_2}{k_1}Ra_\kappa^{-1/2}\right)\left[\frac{R_i}{2HNu_i} + \frac{R_i}{4Hk_w}\ell n\left(\frac{R_o}{R_i}\right)\right] \tag{22}$$

Combining Eqs. (4), (19), and (21) yields

$$\frac{d\theta_0}{dx} = \frac{2}{A^2}\frac{(\theta_1-\theta_0)^3}{\theta_0^2(3\theta_1-2\theta_0)} - B\frac{\theta_0(\theta_1-\theta_0)}{(3\theta_1-2\theta_0)} \tag{23}$$

We have thus attained a relationship between θ_0 and θ_1 in terms of a set of two first-order nonlinear differential equations [Eqs. (4) and (23)]. The dimensionless boundary conditions that complete the mathematical statement of the problem are

At $x = 0$:

$$\theta_0 = 0, \qquad \theta_1 = 1 \tag{24}$$

Before proceeding with the numerical solution, it is worth commenting once more on the major simplifying assumptions inherent in the model just described. These assumptions are common in convection and porous media heat-transfer studies.[2-5,9] However, a brief discussion and justification will add clarity to the presentation. First, the thickness of the porous layer was assumed to be large (infinite) compared to the boundary layer. Considering the fact that the thermal boundary layer is usually very thin, we can conclude that this assumption holds even for moderately thick insulations. Second, in most pipe networks, the pipe length is much greater than the pipe wall thickness. Therefore, the assumption of one-dimensional conduction is justified. Third, the existence of natural convection of the boundary-layer type in insulations and geothermal systems is a proven fact, and considerable research effort has been dedicated to its study, as exemplified by Refs. 2, 4, 5, 9 and references therein.

The system of Eqs. (4), (23), and (24) was solved numerically yielding $\theta_0(x)$ and $\theta_1(x)$. For the numerical solution, the fourth-order Runge-Kutta method was used. However, inspecting the right-hand side of Eq. (3) shows that the first term has a singularity for $\theta_0 = 0$. To deal with this situation, a very small value of θ_0 was used to approximate zero. Regarding the increments in x, it was found necessary to begin the integration with an x increment as small as $\Delta x = 10^{-10}$. As the value θ_0 increased, the effects of the singularity on the integration process disappeared and the value of the x increment was increased to speed up the integration process.

The analysis for the counter-flow configuration is nearly identical to that of the parallel-flow configuration, the only difference being the addition of a minus sign on the left-hand side of Eq. (3). As a result, in the dimensionless equations [Eqs. (4) and (23)], the parameter B needs to be replaced by $-B$ to obtain the differential equations for θ_0 and θ_1 governing the counterflow configuration. The boundary conditions for the counterflow case are

At $x = 0$:

$$\theta_0 = 0 \tag{25a}$$

At $x = 1$:

$$\theta_1 = 1 \tag{25b}$$

The equations governing the counter-flow case were solved by an integration method similar to that for the parallel-flow configuration. However, since the boundary conditions [Eqs. (25)] show that we do not have two conditions at the same x point, a shooting method must be employed to solve these equations. The value of θ_0 at $x = 1$ was guessed, and the integration proceeded from $x = 1$ to $x = 0$. The value of θ_0 was then checked against zero, and the process was repeated, adjusting the guessed value of θ_0 (1) until Eq. (25a) for θ_0 was satisfied. It was found that 1000 equal increments of x between zero and one were sufficient to provide accurate results in the integration.

Results and Discussion

The solution of Eqs. (4) and (23) was carried out for a wide cross section of values for A and B. A summary of the more important results is presented here.

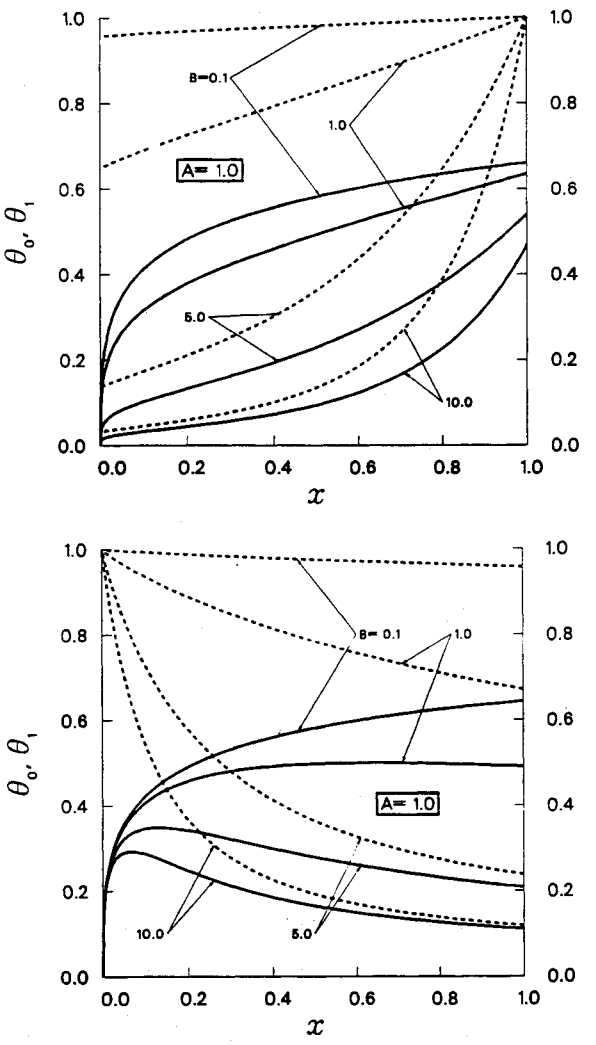

Fig. 2 Temperature profiles for θ_0 (x) ——, and θ_1 (x)---- for characteristic values of B: a) counter-flow and b) parallel flow.

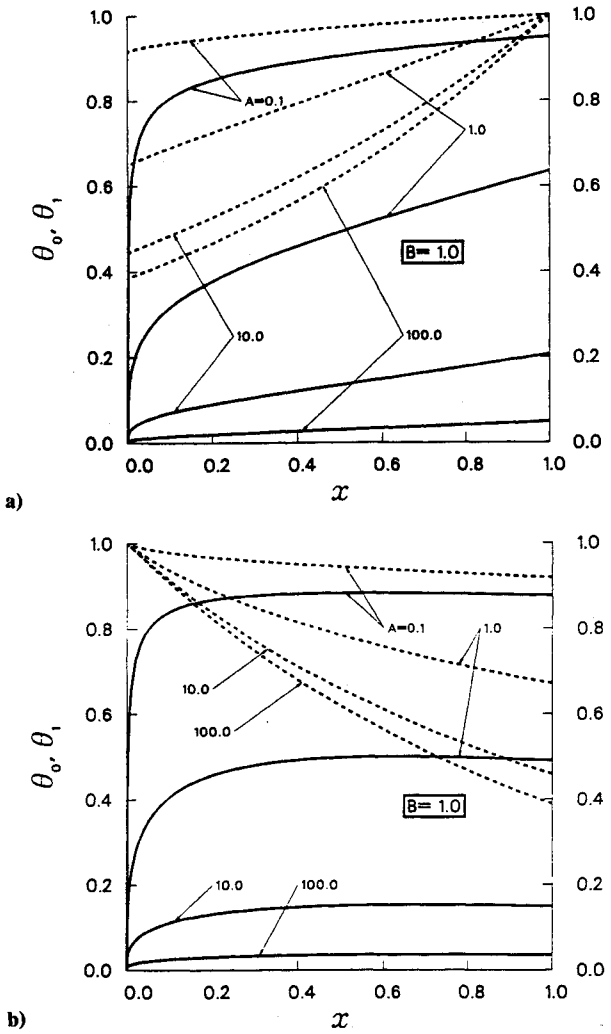

Fig. 3. Temperature profiles for $\theta_0(x)$ ——, and $\theta_1(x)$---- for characteristic values of A: a) counter-flow and b) parallel flow.

Figure 2a pertains to the counter-flow case and shows the variation of the mean temperature of the fluid in the pipe (θ_1) as well as the variation of the temperature of the outer surface of the pipe (θ_0) with distance x, for characteristic values of B. As we move from the pipe inlet ($x = 1$) to the pipe exit ($x = 0$), θ_1 decreases monotonically. This decrease becomes drastic as parameter B increases. On the other hand, as B decreases the dependence of θ_1 on x weakens to the point where for $B = 0.1$, the mean temperature of the fluid in the pipe is practically independent of x and equal to the inlet temperature. By examining Eqs. (6) and (20), one realizes that decreasing B while keeping A constant is equivalent to increasing the Peclet number or the flow rate in the pipe while keeping all of the remaining parameters constant. Increasing the flow rate is then responsible for the reduction of the drop in the fluid temperature along the pipe.

The wall temperature θ_0 decreases monotonically from inlet to outlet (Fig. 2a). As B decreases, the wall temperature increases rapidly (exponentially) over a small distance near the pipe exit ($x = 0$) and weakly thereafter. Except for a small region near the pipe inlet, the local difference between the mean fluid temperature in the pipe θ_1 and the outer wall temperature θ_0 increases at any x as parameter B decreases. Therefore, the local heat transfer is expected to increase with decreasing parameter B.

Figure 2b shows the effect of parameter B for the parallel-flow case. Almost all of the preceding observations made regarding the counter-flow case are valid here as well and will not be repeated for brevity. A new feature, however, is that for high values of B the dependence of θ_0 on x is not monotonic; i.e., θ_0 increases as we move away from the inlet, attains a maximum value, and thereafter decreases. This maximum occurs closer to the inlet as the value of B increases. The reason for the existence of the maximum of θ_0 is that the temperature of the outer wall surface has to increase initially to respond to the heating effect of the fluid in the pipe. As we move downstream, the fluid in the pipe gradually loses its energy, until at it attains the temperature of the cold reservoir ($\theta_1 = 0$). Naturally, the temperature of the pipe wall also shows this trend by starting to decrease until very far from the inlet it also approaches the reservoir temperature.

Figure 3 illustrates the effect of the parameter A. In the counter-flow case (Fig. 3a), increasing A decreases both the mean fluid temperature θ_1 and the wall temperature θ_0 at any given location. As A approaches zero, both θ_0 and θ_1 vary weakly with x. From Eqs. (6) and (20), we see that decreasing parameter A while keeping B constant is equivalent to decreasing the ratio k_2/k_1 or the effective conductivity of the porous material, thus explaining the observed trend. Similar observations are made in Fig. 3b relevant to the parallel-flow case. The maxima on the θ_0 curves, just discussed with reference to Fig. 2b, are again observed.

It is of engineering interest to calculate the effect of both the dimensionless groups in the problem (A and B) on the overall heat flux from the pipe to the surrounding fluid. This is achieved with help of the overall Nusselt number.

$$Nu = \frac{h_o H}{k_2} \tag{26}$$

where the average outer heat-transfer coefficient h_o is defined by

$$h_o = \frac{1}{H}\int_0^H \frac{-k_2\left(\dfrac{\partial T_2}{\partial y^*}\right)_{y^*=0}}{(T_o - T_c)}\,dx^* \tag{27}$$

In dimensionless form, after combining Eqs. (24) and (25), the expression for the Nusselt number is

$$Nu = \frac{Ra_\kappa^{1/2}}{A}\int_0^1 \frac{(\theta_1 - \theta_0)}{\theta_0}\,dx \tag{28}$$

After $\theta_0(x)$ and $\theta_1(x)$ were obtained, Eq. (26) was integrated numerically to yield the value of Nu.

Figure 4 shows that Nu decreases as the parameter A increases. As A approaches zero, the value $Nu = Ra_\kappa^{1/2}$ is attained in both the parallel- and counter-flow cases for all

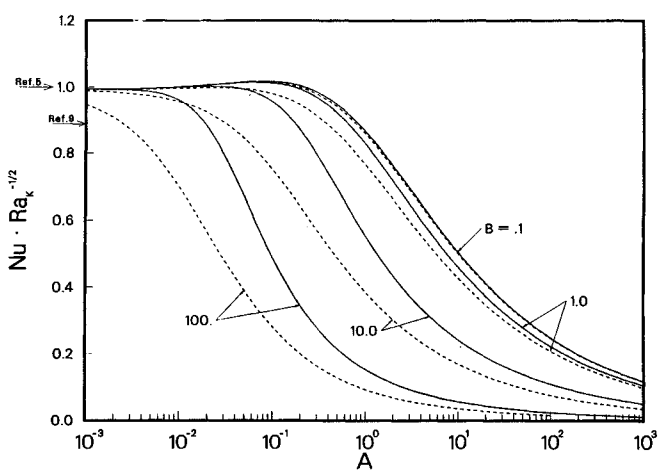

Fig. 4 Heat-transfer results showing the dependence of Nu on the parameters A and B for both counter-flow —— and parallel flow----.

values of B. This value corresponds to natural convection from an isothermal flat plate embedded in a porous medium as obtained using the Oseen linearization.[5] A similarity (exact) solution to this problem was performed by Cheng and Mikowycz[9] yielding $Nu = 0.888\, Ra_\kappa^{1/2}$. In the other extreme, as A becomes very large, the overall heat transfer diminishes for all values of the wall conductivity and therefore the thermal communication between the pipe fluid and the porous material. In all cases, the counter-flow configuration yields a higher overall heat flux than the parallel-flow configuration. This effect, however, weakens as the parameter B decreases, such that for values of $B<0.1$ the overall heat transfer through the pipe is identical for both cases. Note that decreasing B while keeping A constant is equivalent to increasing the flow rate in the pipe.

Conclusions

In this technical Note, a simple yet reliable analysis was presented for the problem of counter-flow and parallel-flow convection in a vertical pipe surrounded by a porous material. Important results revealed interesting features of the temperature distribution of the pipe outer surface, of the mean fluid temperature in the pipe, and of the overall heat flux from the pipe to the surroundings. As the values of parameters A and B approach zero, the outer pipe surface approached an isothermal condition. A maximum was observed in the θ_0 distribution in the parallel-flow case. This maximum is more pronounced and occurs closer to the pipe inlet for larger values of B.

The overall heat flux through the pipe reaches a plateau as A decreases. This plateau corresponds to natural convection from an isothermal vertical wall embedded in a porous medium. The counter-flow configuration yields higher overall heat transfer than for the parallel-flow configuration. This feature diminishes as the pipe flow rate is increased (or the parameter B is decreased).

Acknowledgments

Support for the authors while this research was conducted was provided by the National Science Foundation and by the Microswitch Division of the Honeywell Company.

References

[1]Poulikakos, D., "Interaction Between Film Condensation on One Side of a Vertical Wall and Natural Convection on the Other Side," *Journal of Heat Transfer*, Vol. 108, 1986, pp. 560-66.

[2]Poulikakos, D., and Sura, P., "Conjugate Film Condensation and Natural Convection along the Interface Between a Porous and an Open Space," *International Journal of Heat and Mass Transfer*, Vol. 29, 1986, pp. 1747-1758.

[3]Faghri, M., and Sparrow, E. M., "Parallel-Flow and Counter-Flow Condensation on an Internally Cooled Vertical Tube," *International Journal of Heat and Mass Transfer*, Vol. 23, 1980, pp. 559-562.

[4]Bejan, A., and Anderson, R., "Heat Transfer Across a Vertical Impermeable Partition Imbedded in Porous Medium," *International Journal of Heat and Mass Transfer*, Vol. 24, 1980, pp. 1237-1245.

[5]Bejan, A., and Anderson, R., "Natural Convection at the Interface Between a Vertical Porous Layer and an Open Space," *Journal of Heat Transfer*, Vol. 105, 1983, pp. 124-129.

[6]Weber, J. E., "The Boundary-Layer Regime For Convection in a Vertical Porous Layer," *International Journal of Heat and Mass Transfer*, Vol. 18, 1975, pp. 569-573.

[7]Gill, A. E., "The Boundary-Layer Regime for Convection in a Rectangular Cavity," *Journal of Fluid Mechanics*, Vol. 26, 1966, pp. 515-536.

[8]Libera, J., "Parallel-Flow and Counter-Flow Conjugate Convection from a Vertical Pipe," M.S. Thesis, Univ. of Illinois at Chicago, Chicago, IL, 1989.

[9]Cheng, P., and Mikowycz, W. J., "Free Convection About a Vertical Flat Plate Embedded in a Porous Medium with Applications to Heat Transfer from a Dike," *Journal of Geophysical Research*, Vol. 82, No. 14, 1977, pp. 2040-2044.

Entropy Production in Boundary Layers

Ahmet Selamet* and Vedat S. Arpaci†
University of Michigan, Ann Arbor, Michigan 48109

Introduction

THE interpretation of the contemporary problems of thermomechanics in terms of entropy production is lately receiving increased attention. Because of its size, no attempt will be made here to survey the literature (see, for example, Bejan[1,2] for applications involving heat transfer and Arpaci[3,4] and Arpaci and Selamet[5,6] for applications involving radiation and flames). The following brief review on the local entropy production is for later convenience.

The development of the entropy production in moving media requires the consideration of the momentum, energy, and entropy balances. The fundamental difference,

$$\text{Total energy} - (\text{Momentum})\mathrm{v}_i - (\text{Entropy})T \tag{1}$$

may be rearranged to yield

$$\rho\left(\frac{Du}{Dt} - T\frac{Ds}{Dt} + p\frac{D\mathrm{v}}{Dt}\right) = -\left(\frac{q_i}{T}\right)\frac{\partial T}{\partial x_i} + \tau_{ij}s_{ij} + u''' - Ts''' \tag{2}$$

where s_{ij} is the rate of deformation. For a reversible process, all forms of dissipation vanish, and

$$\left(\frac{Du}{Dt} - T\frac{Ds}{Dt} + p\frac{D\mathrm{v}}{Dt}\right) = 0 \tag{3}$$

which is the Gibbs Thermodynamic relation. For an irreversible process, Eq. (3) continues to hold provided the process can be assumed in local equilibrium. Then, the local entropy production is found to be

$$s''' = \frac{1}{T}\left[-\left(\frac{q_i}{T}\right)\left(\frac{\partial T}{\partial x_i}\right) + \tau_{ij}s_{ij} + u'''\right] \tag{4}$$

where the first term in brackets denotes the dissipation of thermal energy into entropy (lost heat), the second term denotes the dissipation of mechanical energy into heat (lost work), and the third term denotes the dissipation of any (except thermomechanical) energy into heat. When radiation is appreciable, q_i denotes the total flux involving the sum of the conductive flux and the radiative flux

$$q_i = q_i^K + q_i^R \tag{5}$$

Neglecting contribution of viscous dissipation and assuming conductive and radiative heat fluxes to be in the transversal direction, Eq. (4) may be rearranged as

$$s''' = -\frac{1}{T^2}(q_y^K + q_y^R)\left(\frac{\partial T}{\partial y}\right) \tag{6}$$

Foregoing general considerations are applied below to a forced convection boundary layer.

Received Jan. 27, 1989; revision received July 5, 1989.

*Assistant Research Scientist. Dept of Mechanical Engineering and Applied Mechanics.

†Professor, Dept. of Mechanical Engineering and Applied Mechanics.